Combustion and Flame 213 (2020) 467–474

Contents lists available at ScienceDirect

Combustion and Flame

journal homepage: www.elsevier.com/locate/combustflame

Mixture rules and falloff are now major uncertainties in experimentally derived rate parameters for H + O_2 (+M) ↔ HO_2 (+M)

Lei Lei[a], Michael P. Burke[a,b,*]

[a] Department of Mechanical Engineering, Columbia University, New York, NY 10027, United States
[b] Department of Chemical Engineering, Data Science Institute, Columbia University, New York, NY 10027, United States

ARTICLE INFO

Article history:
Received 18 October 2019
Revised 26 November 2019
Accepted 27 November 2019
Available online 3 January 2020

Keywords:
mixture rules
pressure-dependent reactions
master equation

ABSTRACT

Rate constants for the title reaction for different bath gas species, M, are essential to accurate combustion predictions. Most experimental studies of the title reaction assume the reaction is in the low-pressure limit. Furthermore, experimental studies for M = H_2O usually rely on measurements in H_2O/*A* mixtures, separate measurements in a reference bath gas M = *A*, and an assumed mixture "rule," which estimates rate constants in the mixture from those of pure bath gases. We present results from master equation calculations to quantify the uncertainties due to these assumptions in experimental interpretations. Our calculations indicate potential errors due to falloff and mixture rule assumptions that would be imperceptible experimentally over typical variations of pressure and composition yet introduce substantial uncertainties (reaching ~50%) in reported rate constants, which often involve extrapolation to zero pressure and unity mole fraction. Going forward, we recommend that experimentally determined pseudo-second-order rate constants for H + O_2 ↔ HO_2 for the experimental pressure and mixture composition (which are independent of these assumptions) be reported, that experiments used to derive rate constants in the low-pressure limit or for M = H_2O be conducted at lower pressures and higher H_2O fractions (where these assumptions are more accurate), and that uncertainty analysis consider uncertainties due to falloff and mixture rule assumptions.

1. Introduction

The title reaction is among the most important reactions in combustion. Given that it competes with main chain branching reaction, H + O_2 = OH + O, it may be the most important pressure-dependent reaction. Indeed, their competition plays a key role in the H_2/O_2 explosion limits [1–3] and, more generally, many combustion properties for all fuels [4–6].

Since the early studies of combustion kinetics [1–3], the reaction has been known to proceed via a rovibrationally excited HO_2 complex that is stabilized through energy-transferring collisions with the surrounding "bath gas" molecules (i.e. the Lindemann–Hinshelwood mechanism [7,8]). The rate constant, $k_i(T, P)$, depends on pressure, *P*, because the collision rate depends on pressure. Similarly, it also depends on the bath gas species, *i*, (i.e. $k_i(T, P)$), or more generally the bath gas mixture composition, $\underline{X}$, (i.e. $k(T, P, \underline{X})$), because the collision frequency and amount of energy transferred per collision depend on the molecular characteristics of the bath gas/complex pair [9–14].

Determining $k_i(T, P)$ for the major species in combustion mixtures has been a major research focus since the infancy of combustion kinetics [11,15–27] – for both direct use in kinetic models and understanding microscopic energy transfer mechanisms. Other than N_2 and O_2, H_2O is probably the most important bath gas species, given that it is a major combustion product, is a major diluent in Exhaust Gas Recirculation (EGR) [28] and Moderate or Intense Low-oxygen Dilution (MILD) [29] strategies, and is especially effective in stabilizing HO_2 [11,16–24].

Nearly all experimental studies devoted to determining $k_{H_2O}(T, P)$ rely on $k(T, P, \underline{X})$ measurements in H_2O/*A* mixtures with H_2O mole fractions $X_{H_2O} \approx$ 5–25%, $k_A(T, P)$ measurements, and an assumed mixture "rule" [16–24]. The classic linear mixture rule [30]

$$k_{\text{LMR-P}}(T, P, \underline{X}) = \sum_{i=1}^{M} k_i(T, P) X_i \tag{1}$$

is the most commonly used mixture rule, such that $k_{H_2O}(T, P)$ is determined via

$$k_{H_2O,\text{LMR-P}}(T, P) = \frac{k(T, P, \underline{X}) - k_A(T, P) X_A}{X_{H_2O}} \tag{2}$$

* Corresponding author at: 220 Mudd Building MC 4703; 500 W. 120th St; New York, NY 10027, United States.
E-mail address: mpburke@columbia.edu (M.P. Burke).

https://doi.org/10.1016/j.combustflame.2019.11.041
0010-2180/

Furthermore, most studies [16–20,22,24] (including the three highlighted here [20,22,24]) also assume $k(T, P, \underline{X})$ is in its low-pressure limit,

$$k_0(T, \underline{X}) = \lim_{P\to 0} k(T, P, \underline{X})/[M] \quad (3)$$

at the experimental P yielding an "effective" low-pressure limit,

$$k_{0\text{-eff}}(T, P, \underline{X}) = k(T, P, \underline{X})/[M] \quad (4)$$

such that

$$k_{H_2O,0\text{-eff,LMR-P}}(T, P, \underline{X}) = \frac{k_{0\text{-eff}}(T, P, \underline{X}) - k_{A,0\text{-eff}}(T, P)X_A}{X_{H_2O}} \quad (5)$$

is then calculated and reported. (Note that this is implicitly what occurs in combustion codes [31,32] if $k_{H_2O,0\text{-eff}}$ is fit to experimental data using a kinetic model containing separate expressions reading "H + O_2 + A = HO_2 + A" and "H + O_2 + H_2O = HO_2 + H_2O").

In reality, the dependence of rate constants on mixture composition is generally not linear [30,33–36]. In fact, this was realized around the time when collider-specific effects first became a major topic of study (e.g. [9,10] and references therein); and, consequently, understanding the dependence of rate constants on mixture composition was a major topic of study about half a century ago. While these studies revealed that the dependence of rate constants on the mixture composition was not strictly linear at pressures below the high-pressure limit, the magnitude of these effects was generally found to be relatively small (e.g. ~10-20% in the low pressure limit for typical single-channel reactions [33]) compared to experimental precision *at that time*.

The observation that mixture rule errors were less than experimental precision at the time of those studies five decades ago likely contributed to a now outdated, but still prevailing, notion that the linear mixture rule introduces negligible uncertainty. For example, mixture rules are not usually considered in experimental [16–24] or computational [28,37–39] uncertainty analysis.

The systematic errors from mixture rules on experimental interpretations are now worth revisiting for two reasons. First, drastic improvements in experimental methods for kinetics experiments (e.g. [40]) over the period since most previous mixture studies have resulted in an impressive level of precision – on the order of ~10–20% for rate constants of H + O_2 (+M) = HO_2 (+M) [22,24]. Second, our recent studies have revealed much larger deviations from the classic linear mixture rule in the intermediate falloff regime than the ~10–20% found for single-channel reactions in the low-pressure limit [33] – reaching ~60% for single-channel reactions [34] and a factor of ~10 for multi-channel reactions [35,36]. Indeed this question, together with falloff effects, was discussed after the authors' presentation on mixture effects at the 2018 Flame Chemistry Workshop, raised by Juergen Troe after [24] at the 2018 Combustion Symposium, and pointed out in a recent paper [41].

Here, we address this question at the conditions of three experimental studies [20,22,24] using a master equation (ME) model that is entirely consistent with the experimental data [20,22,24] but does not involve any assumptions of low-pressure limit rate constants or mixture rules. Because deviations from mixture rules are sensitive to pressure (i.e. the extent of falloff), this question can only be explored considering both falloff and mixture effects simultaneously, as done here. We then also use this ME model to estimate uncertainties due to both assumptions across wide ranges of pressure and composition – to serve as a guide for selection of future experimental conditions to derive $k_{A,0}(T)$ and $k_{H_2O,0}(T)$.

2. Methodology

2.1. Master equation calculations in PAPR-MESS

Ab initio master equation (ME) calculations are performed for the title reaction using a 1D-ME model in PAPR-MESS [42] based on the multi-reference variable reaction coordinate transition state theory (VRC-TST) calculations of Harding et al. [43]. The collisional energy transfer function is described by the common exponential down model [12], where the probability of a "down" collision of HO_2 with initial energy E by i yielding HO_2 with a (lower) final energy E' is given by $P_i(E', E) = \frac{1}{N_i}\exp[-(E-E')/\langle\Delta E_d\rangle_i)]$ for $E > E'$, with N_i being the normalization factor; the probability function for "up" collisions, $P_i(E', E)$ for $E < E'$, is obtained via detailed balance. Collision frequencies for HO_2-H_2O were calculated based on a dipole-dipole collision frequency [11,44], as recommended for HO_2-H_2O elsewhere [11,18,22] (cf. Supplemental Material). Collision frequencies for all other HO_2-bath pairs use the Lennard Jones model. The parameters, A_i and n_i, describing average energies transferred per down collision via $\langle\Delta E_d\rangle_i = A_i(T/298)^{n_i}$ for each i are chosen such that ME calculations of $k(T, P, \underline{X})$ together with Eqs. (4) and (5) reproduce $k_{i,0\text{-eff}}(T, P)$ and $k_{i,0\text{-eff,LMR-P}}(T, P, \underline{X})$ reported in experimental studies from Michael et al. [22] and Shao et al. [24] at corresponding conditions.

2.1.1. Reproducing reported data at 296 K

The rate constants reported by Michael et al. [22] were determined at a temperature of 296 K. Experimental pressures were varied from 25 to 200 Torr for pure O_2 and mixtures of Ar/O_2 and N_2/O_2; and experimental pressures were varied from 2.2 to 7.0 Torr for H_2O/O_2 mixtures. The mixture composition for i/O_2 mixtures where i = Ar, N_2 is taken to be $X_i = 0.985$ and $X_{O_2} = 0.015$; and the mixture composition for H_2O/O_2 mixtures is taken to be $X_{H_2O} = 0.1$ and $X_{O_2} = 0.9$ (consistent with that reported in the experimental study [22]).

At 296 K, the dipole-dipole collision frequency for HO_2-H_2O system is calculated to be $7.37 \times 10^{-10}\text{cm}^3\text{s}^{-1}$, which can be effectively reproduced in PAPR-MESS [42] using the (fictitious) parameters $\sigma_{H_2O} = 2.673$ Å [45] and $\epsilon_{H_2O} = 6360.64\,\text{cm}^{-1}$ within a Lennard Jones model. The exponential-down factors are chosen such that the ME calculated rate constants match those reported in [22] at a representative pressure of 100 Torr for pure O_2 and mixtures of Ar/O_2 and N_2/O_2 and of 5 Torr for H_2O/O_2 mixtures (roughly the midpoint of the experimental pressure ranges).

For $A = O_2$, $k_{A,0\text{-eff}}(T, P)$ is calculated from the ME results for $k(T, P, \underline{X})$ via Eq. (4); and for all i in i/O_2 mixtures, $k_{i,0\text{-eff,LMR-P}}(T, P, \underline{X})$ is calculated from the ME results for $k(T, P, \underline{X})$ via Eqs. (4) and (5). Exponential-down factors are first chosen for $A = O_2$ such that the calculated $k_{O_2,0\text{-eff}}(T, P)$ (shown in the third column of Table 1) matches the experimentally reported $k_{O_2,0\text{-eff,exp}}(T, P)$ (shown in

Table 1
Exponential-down factors in 1D-ME that reproduce reported data at 296 K.

	$k_{i,0\text{-eff,LMR-P,exp}}(T, P, \underline{X})$[a]	$k_{i,0\text{-eff,LMR-P}}(T, P, \underline{X})$[b]	$\langle\Delta E_d\rangle_i(T)$[c]
O_2[d]	3.1	3.10	35.03
Ar/O_2[d,f]	2.2	2.20	30.71
N_2/O_2[d,f]	4.3	4.30	40.13
H_2O/O_2[e,f]	50	49.69	101.77

[a] from [22], units: 10^{-32} $\text{cm}^6\text{molec}^{-2}\text{s}^{-1}$;
[b] calculated using PAPR-MESS, units: 10^{-32} $\text{cm}^6\text{molec}^{-2}\text{s}^{-1}$;
[c] the listed exponential-down factors in i/O_2 mixtures are for i, units: cm^{-1};
[d] calculated at 100 Torr;
[e] calculated at 5 Torr;
[f] X_i/X_{O_2} = 98.5%/1.5% for i = Ar, N_2; X_i/X_{O_2} = 10%/90% for $i = H_2O$.

Table 2
Exponential-down factors in 1D-ME that reproduce reported data at 1200 K.

	$k_{i,0\text{-eff,LMR-P,exp}}(T,P,\underline{X})$[a]	$k_{i,0\text{-eff,LMR-P}}(T,P,\underline{X})$[b]	$\langle\Delta E_d\rangle_i(T)$[c]
Ar	4.93	4.93	162.85
N_2	6.82	6.82	186.15
H_2O/Ar[d]	113	112.82	862.33

[a] from [24], units: 10^{-33} $cm^6molec^{-2}s^{-1}$;
[b] calculated using PAPR-MESS, units: 10^{-33} $cm^6molec^{-2}s^{-1}$;
[c] the listed exponential-down factors in *i*/Ar mixtures are for *i*, units: cm^{-1};
[d] $X_{H_2O}/X_{Ar} = 10\%/90\%$.

the second column of Table 1). Using these exponential-down factors for $A = O_2$, exponential-down factors for i = Ar, N_2, and H_2O are then chosen such that the calculated $k_{i,0\text{-eff,LMR-P}}(T,P,\underline{X})$ (also shown in the third column of Table 1) match $k_{i,0\text{-eff,LMR-P,exp}}(T,P,\underline{X})$ (also shown in the second column of Table 1) in each of the mixtures. The last column in Table 1 summarizes the obtained $\langle\Delta E_d\rangle_i$ for O_2, Ar, N_2 and H_2O at 296 K in the 1D-ME model.

2.1.2. Reproducing reported data at 1200 K

A similar procedure is performed for 1200 K and 15 atm, representative of the experimental conditions of Shao et al. [24]. Experimental values at 1200 K (shown in the second column of Table 2) are first calculated from the reported Arrhenius expressions in [24]. The mixture composition for H_2O/Ar mixtures is taken to be $X_{H_2O} = 0.1$ and $X_{Ar} = 0.9$ (within the reported range experimentally); the determinations for Ar and N_2 are assumed to be for pure bath gases. The ME calculations (shown in the third column of Table 2) are performed at a representative pressure of 15 atm for Ar, N_2, and H_2O/Ar mixtures.

At 1200 K, the dipole-dipole collision frequency for HO_2-H_2O system is calculated to be $8.62 \times 10^{-10} cm^3s^{-1}$, which can be effectively reproduced in PAPR-MESS [42] by using the (fictitious) parameters $\sigma_{H_2O} = 2.673$ Å [45] and $\epsilon_{H_2O} = 6479.91\ cm^{-1}$ within a Lennard Jones model. The results are presented in Table 2 for the 1D-ME model.

2.1.3. Testing consistency with reported data at 800 K

After the parameters, A_i and n_i, within $\langle\Delta E_d\rangle_i = A_i(T/298)^{n_i}$ for each i were chosen such that ME calculations of $k(T, P, \underline{X})$ together with Eqs. (4) and (5) reproduce $k_{i,0\text{-eff}}(T, P)$ and $k_{i,0\text{-eff,LMR-P}}(T,P,\underline{X})$ reported at 296 K [22] and 1200 K [24] (and corresponding pressure and mixture conditions), the results from this ME model were then tested against the reported $k_{i,0\text{-eff,exp}}(T, P)$ and $k_{i,0\text{-eff,LMR-P,exp}}(T,P,\underline{X})$ from Ashman and Haynes [20] at 800 K and 1 atm. The values for $k_{i,0\text{-eff}}(T, P)$ and $k_{i,0\text{-eff,LMR-P}}(T,P,\underline{X})$ calculated by the ME model, together with Eqs. (4) and (5), reproduced the reported values within 13% – well within the reported uncertainties of 30%, such that the ME model is also consistent with the reported data at 800 K.

2.2. Master equation calculations in Variflex

Since all one-dimensional ME models make assumptions in the treatment of angular momentum, additional calculations were performed using alternative assumptions in the treatment of angular momentum – to test the sensitivity of the derived results to the assumptions regarding angular momentum. Here, ab initio ME calculations are also performed for the title reaction using a 2D/φ-ME model [12] (which makes different assumptions about angular momentum transfer) in Variflex [46] based on the VRC-TST calculations of Selleväg et al. [15].

Similar procedures are repeated for the 2D/φ-ME model to derive the parameters, A_i and n_i, for each i in the 2D/φ-ME model such that the 2D/φ-ME model also reproduces reported data. The procedures are otherwise identical to those above for the 1D-ME model except for the following modification: (due to the lack of functionality to handle bath gas mixtures in Variflex, the code which implements the 2D/φ-ME model) the exponential-down factors are instead chosen such that the calculated $k_{i,0\text{-eff}}(T, P)$ match the reported $k_{i,0\text{-eff,LMR-P,exp}}(T,P,\underline{X})$ from the experiments (i.e. assuming experiments were conducted in only pure mixtures). The equivalent tables to Tables 1 and 2 are provided as Table S5 and S6 in the Supplemental Material.

It is worth noting that with the 2D/φ-ME calculations, it is not possible to reach the experimentally reported rate constants for H_2O at both 296 and 1200 K even in the strong-collision limit and even when using the dipole-dipole collision frequency. However, comparison of the 1D-ME and 2D/φ-ME model results for O_2, Ar, and N_2 can be used to assess the differences in the estimated extent of falloff (which also affects estimates of deviations from LMR,P).

Of course, full 2D-ME calculations [13,47] would allow proper treatment of angular momentum but insufficient data are available to implement such a treatment for the mixtures considered here. Nevertheless, full a priori 2D-ME calculations [5,48], which are available for Ar as the bath gas, are used here as another point of comparison for Ar to assess differences in the predicted extent of falloff among ME models.

3. Results and discussion

Ultimately, the methodology described in the previous section yields a 1D-ME model that is entirely consistent with the experimental data [20,22,24] but does not involve any assumptions of low-pressure limit rate constants or mixture rules. This 1D-ME model is then used to assess the potential errors due to the low-pressure limit and linear mixture rule assumptions in previous and future experimental interpretations.

3.1. Interpretations of previous experiments

Results from the ME calculations are presented in Table 3 for experimental conditions representative of previous experiments at 296 K and ~5 Torr [22], 800 K and 1 atm [20], and 1200 K and ~15 atm [24]. While $k(T, P, \underline{X})$ is directly calculated from the ME, all other quantities are calculated from $k(T, P, \underline{X})$ and Eqs. (1)–(5). Values are presented across a range of H_2O mole fractions in H_2O/*A* mixtures from 0.0 to 1.0, where $X_{H_2O} = 0.0$ corresponds to pure *A* and $X_{H_2O} = 1.0$ corresponds to pure H_2O. Note that the italicized values roughly correspond to the range of mixtures considered experimentally ($X_{H_2O} \approx 0.0$ to 0.2) whereas the non-italicized values are outside the experimental ranges. Results are shown for the 1D-ME for all mixtures; results are shown for the 2D/φ-ME model for pure O_2, N_2, and Ar only and an a priori 2D-ME for Ar only. As such, the results discussed below refer to those from the 1D-ME model, unless otherwise noted.

The first two rows for each *T*/*P*/*A*, $k_{0\text{-eff}}(T, P, \underline{X})$ and $k_{H_2O,0\text{-eff,LMR-P}}(T,P,\underline{X})$, correspond to what is generally reported in most experimental studies. Specifically, $k_{0\text{-eff}}(T, P, \underline{X})$ for $X_{H_2O} = 0.0$ would usually correspond to the value reported for *A* and $k_{H_2O,0\text{-eff,LMR-P}}(T,P,\underline{X})$ for $X_{H_2O} = 0.1$ (roughly the midpoint of many experimental ranges of X_{H_2O}) would usually correspond to the value reported for H_2O. The values indicated by "d" and "e" superscripts are, in fact, exactly the values reported since the energy-transfer parameters in the ME model were chosen to match these values. Again, the "0-eff" and "LMR-P" subscripts denote that the reported values are not necessarily the actual low-pressure limit or pure H_2O values but rather the derived values if one were to make the low-pressure limit and linear mixture rule assumptions. Eqs. (4) and (5) can be inverted from $k_{0\text{-eff}}(T, P, \underline{X})$ and

Table 3
Results for conditions representative of [22], [20], and [24].

	1D-ME model						2D/φ-ME model	2D-ME model[g]
X_{H_2O}	*0.00*	*0.05*	*0.10*	*0.20*	0.50	1.00	*0.00*	*0.00*
H_2O / O_2 at 296 K and 5 Torr								
$k_{0\text{-eff}}(T, P, \underline{X})$[a]	*3.20*	*5.55*	*7.85*	*12.40*	25.84	47.90	*3.20*	–
$k_{H_2O,0\text{-eff,LMR-P}}(T, P, \underline{X})$[a]	–	*50.14*	*49.69*[d]	*49.18*	48.48	47.90	–	–
$k(T, P, \underline{X})$[b]	*5.22*	*9.05*	*12.80*	*20.22*	42.15	78.14	*5.22*	–
$k_0(T, \underline{X})$[a]	*3.21*	*5.57*	*7.88*	*12.47*	26.11	48.76	*3.21*	–
$k_{0\text{-eff}}(T, P, \underline{X})/k_0(T, \underline{X})$	***1.00***	***1.00***	***1.00***	***0.99***	***0.99***	**0.98**	***1.00***	–
$k(T, P, \underline{X})/k_{LMR\text{-P}}(T, P, \underline{X})$	*1.00*	*1.02*	*1.02*	*1.02*	1.01	1.00	*1.00*	–
$k_{H_2O,LMR\text{-P}}(T, P)/k_{H_2O}(T, P)$	–	***1.05***	***1.04***	***1.03***	**1.01**	**1.00**	–	–
$k_{H_2O,0\text{-eff,LMR-P}}(T, P, \underline{X})/k_{H_2O,0}(T)$	–	*1.03*	*1.02*	*1.01*	0.99	0.98	–	–
H_2O / N_2 at 800 K and 1 atm								
$k_{0\text{-eff}}(T, P, \underline{X})$[a]	*1.39*	*2.38*	*3.32*	*5.10*	10.02	17.39	*1.35*	–
$k_{H_2O,0\text{-eff,LMR-P}}(T, P, \underline{X})$[a]	–	*21.21*	*20.67*	*19.94*	18.65	17.39	–	–
$k(T, P, \underline{X})$[c]	*1.27*	*2.18*	*3.04*	*4.68*	9.19	15.96	*1.24*	–
$k_0(T, \underline{X})$[a]	*1.53*	*2.65*	*3.74*	*5.87*	12.12	22.41	*1.37*	–
$k_{0\text{-eff}}(T, P, \underline{X})/k_0(T, \underline{X})$	***0.91***	***0.90***	***0.89***	***0.87***	**0.83**	**0.78**	***0.98***	–
$k(T, P, \underline{X})/k_{LMR\text{-P}}(T, P, \underline{X})$	*1.00*	*1.09*	*1.11*	*1.11*	1.07	1.00	*1.00*	–
$k_{H_2O,LMR\text{-P}}(T, P)/k_{H_2O}(T, P)$	–	***1.22***	***1.19***	***1.15***	**1.07**	**1.00**	–	–
$k_{H_2O,0\text{-eff,LMR-P}}(T, P, \underline{X})/k_{H_2O,0}(T)$	–	*0.95*	*0.92*	*0.89*	0.83	0.78	–	–
H_2O / Ar at 1200 K and 15 atm								
$k_{0\text{-eff}}(T, P, \underline{X})$[a]	*0.49*[e]	*1.06*	*1.57*	2.50	4.89	8.17	*0.49*	*0.40*
$k_{H_2O,0\text{-eff,LMR-P}}(T, P, \underline{X})$[a]	–	*11.86*	*11.28*[e]	10.54	9.29	8.17	–	–
$k(T, P, \underline{X})$[c]	*4.51*	*9.72*	*14.41*	22.94	44.86	74.90	*4.51*	*3.65*
$k_0(T, \underline{X})$[a]	*0.65*	*1.45*	*2.21*	3.70	8.08	15.29	*0.52*	*0.47*
$k_{0\text{-eff}}(T, P, \underline{X})/k_0(T, \underline{X})$	***0.76***	***0.73***	***0.71***	**0.68**	**0.61**	**0.53**	***0.94***	***0.84***
$k(T, P, \underline{X})/k_{LMR\text{-P}}(T, P, \underline{X})$	*1.00*	*1.21*	*1.25*	1.23	1.13	1.00	*1.00*	*1.00*
$k_{H_2O,LMR\text{-P}}(T, P)/k_{H_2O}(T, P)$	–	***1.45***	***1.38***	**1.29**	**1.14**	**1.00**	–	–
$k_{H_2O,0\text{-eff,LMR-P}}(T, P, \underline{X})/k_{H_2O,0}(T)$	–	*0.78*	*0.74*	0.69	0.61	0.53	–	–

[a] 10^{-32} $cm^6 molec^{-2} s^{-1}$;
[b] 10^{-15} $cm^3 molec^{-1} s^{-1}$;
[c] 10^{-13} $cm^3 molec^{-1} s^{-1}$;
[d,e] Values are used to fit $\langle \Delta E_d \rangle_i$ at [d]296 K to reported $k_{H_2O,0\text{-eff,LMR-P}}$ [22] and [e]1200 K to reported Arrhenius fits for $k_{Ar,0\text{-eff}}$ and $k_{H_2O,0\text{-eff,LMR-P}}$ [24];
[f] Values in italics roughly correspond to experimental ranges of X_{H_2O};
[g] Calculated via PLOG fits of data from [5] for Ar only.

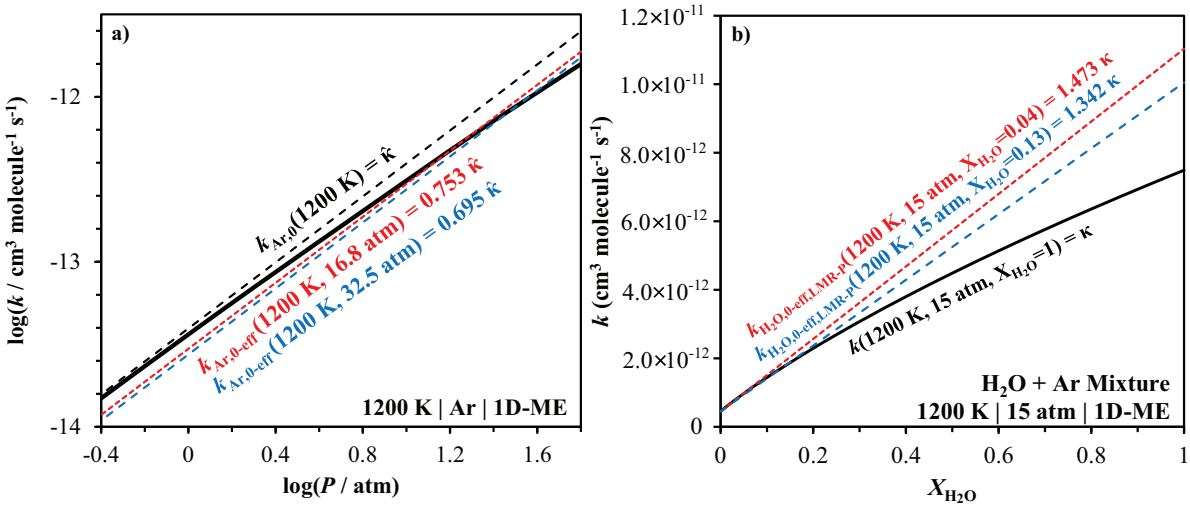

Fig. 1. Variation in $k_{Ar,0\text{-eff}}(T, P)$ (a, where $\hat{\kappa} = 6.45 \times 10^{-33}$ cm^6 $molec^{-2}$ s^{-1}) and $k_{H_2O,LMR\text{-P}}(T, P, \underline{X})$ (b, where $\kappa = 7.49 \times 10^{-12}$ cm^3 $molec^{-1}$ s^{-1}) over the ranges of experimental conditions considered in [24].

$k_{H_2O,0\text{-eff,LMR-P}}(T, P, \underline{X})$ to give $k(T, P, \underline{X})$, which is the value of the pseudo-second-order rate constant (i.e. that for H + O_2 ↔ HO_2) from the experiment, presented in the third row of the table.

The fourth row of the table displays the "actual" low-pressure limit rate constant, $k_0(T, \underline{X})$, according to the 1D-ME model calculated by inserting ME results for $k(T, P, \underline{X})$ at decreasing P into Eq. (3) to evaluate the $P \to 0$ limit. The "actual" low-pressure limit rate constant, corresponding to the $P \to 0$ limit, can be contrasted with the effective low-pressure limit rate constant, $k_{0\text{-eff}}(T, P, \underline{X})$, corresponding to the experimental P (e.g. Fig. 1). Their ratio (highlighted in bold), $k_{0\text{-eff}}(T, P, \underline{X})/k_0(T, \underline{X})$, presented in the fifth row, can then be interpreted as the deviation from the low-pressure limit for a given temperature, pressure, and mixture estimated by the 1D-ME model.

The sixth row, $k(T, P, \underline{X})/k_{LMR\text{-P}}(T, P, \underline{X})$, is the deviation of the rate constant in the mixture estimated by the classic linear mixture rule (LMR,P) from that calculated by the 1D-ME model. The seventh row, $k_{H_2O,LMR\text{-P}}(T, P)/k_{H_2O}(T, P)$, is then the error in extracting $k_{H_2O}(T, P)$ from $k(T, P, \underline{X})$ via the linear mixture rule (LMR,P). As depicted in Fig. 1, the errors in extracting $k_{H_2O}(T, P)$ from $k(T,$

P, $\underline{X}$) via LMR,P are larger than the deviations from LMR,P because the errors in extracting $k_{H_2O}(T, P)$ involve extrapolation from $X_{H_2O} = 0.1$ (of the experiments) to $X_{H_2O} = 1.0$ (pure H_2O). The final row, $k_{H_2O,0\text{-eff,LMR-P}}(T, P, \underline{X})/k_{H_2O,0}(T)$, is the error in extracting the low-pressure limit rate constant for pure H_2O, $k_{H_2O,0\text{-eff,LMR-P}}(T, P, \underline{X})$, from $k(T, P, \underline{X})$ due to both the low-pressure limit and linear mixture rule assumptions.

Interestingly, the estimated errors due to the low-pressure limit assumption (indicated in bold), $k_{0\text{-eff}}(T, P, \underline{X})/k_0(T, \underline{X})$, of ~5%, ~10-15%, and ~30% for the experimental conditions representative of [20,22], and [24] are comparable to reported uncertainties of 3–10%, 30%, and 12–19%. Similarly, the errors due to the assumed mixture rule in deriving H_2O-specific rate constants, $k_{H_2O}(T, P)$, from $k(T, P, \underline{X})$, (indicated in bold) of ~5%, ~15-20%, and ~40-45% for conditions representative of [20,22], and [24] are also comparable to reported uncertainties. While it may initially seem surprising that the potential errors in the reported $k_{i,0}(T)$'s could be comparable to and/or exceed experimental precision, it is worth noting that the variation in $k_{i,0\text{-eff}}(T, P)$ and $k_{H_2O,0\text{-eff,LMR-P}}(T, P, \underline{X})$ over the experimental ranges of pressure and H_2O mole fraction is typically less than the experimental precision – with $k_{Ar,0\text{-eff}}(1200\,\text{K}, 16.8\,\text{atm})$ and $k_{Ar,0\text{-eff}}(1200\,\text{K}, 32.5\,\text{atm})$ differing by only ~8% and $k_{H_2O,0\text{-eff,LMR-P}}(1200\,\text{K}, 15\,\text{atm}, X_{H_2O} = 0.04)$ and $k_{H_2O,0\text{-eff,LMR-P}}(1200\,\text{K}, 15\,\text{atm}, X_{H_2O} = 0.14)$ differing by only ~9% (Fig. 1) – such that these potential errors, while significant, would be imperceptible experimentally.

It would be tempting to say that the 1D-ME model results could be used to correct for the errors due to assumptions in the experimental interpretations. The "corrected" values would correspond to the underlined values in Table 3, which are the low-pressure limit values for pure Ar and pure H_2O, $k_{0,Ar}(T)$ and $k_{0,H_2O}(T)$, calculated by the 1D-ME.

However, additional 2D/φ-ME calculations and a priori 2D-ME results [5,48] suggest that exact quantification of falloff effects (and, correspondingly, mixture effects) depends on the treatment of angular momentum (cf. the final two columns of Table 3 and Supplemental Material). For example, the three ME models all suggest different corrections to the low-pressure limit rate constants for Ar at 1200 K – the 1D-ME, 2D/φ-ME, and a priori 2D-ME calculations yield $k_{0\text{-eff}}(T, P, \underline{X})/k_0(T, \underline{X})$ values of 0.76, 0.94, and 0.84, respectively. With mixture rule deviations being sensitive to falloff [34], the errors due to the classic linear mixture rule assumption can likewise be expected to depend on the treatment of angular momentum. Therefore, any quantitative corrections to reported experimental quantities for H_2O must await mixture analysis using an a priori 2D-ME, which has yet to be attempted for any reaction. Altogether, these results suggest that it would be most appropriate to think of the 1D-ME results as simply an alternative interpretation of the experimental data (and an indication of the additional uncertainties in the experimental interpretations due to assumptions in the analysis).

Combining Arrhenius fits of k_∞(T), the high-pressure limit rate constant [43], Arrhenius fits of $k_{i,0}(T)$ for each i from the 1D-ME calculations evaluated via Eq. (3), and fits for the centering factor, $F_{c,i}$, of $k_i(T, P)$ for each i from 1D-ME calculations across various pressures within the standard Troe formula [49] yields the representation of the 1D-ME model in Table 4.

In theory, the above expressions would be best implemented using our nonlinear reduced-pressure-based mixture rule [34–36] (NMR,R, within ~3% for the title reaction [34]) along with the present $Z_i(T)$ and $\langle\Delta E_d\rangle_i(T)$ for each i, as reported in Table 5. The expressions could also be implemented (with reasonable, albeit less, accuracy) using our linear reduced-pressure-based mixture rule [34–36] (LMR,R, within ~10% for the title reaction [34]). However, neither of these two recently proposed mixture rules are available yet in combustion codes. Most combustion codes would either implement the above expressions using the classic linear mixture rule (LMR,P) or no mixture rule – introducing ~60% or factor of three uncertainties in $k(T, P, \underline{X})$, respectively.

Table 4
Separate Troe expressions of 1D-ME calculations for Ar, N_2, and H_2O.

Ar	$k_{Ar,0}(T)^a = 1.26 \times 10^{-27} T^{-1.67} \exp(-438.48\ \text{K}/T)$ $k_\infty(T)^b = 2.04 \times 10^{-12} T^{0.58} \exp(107.57\ \text{K}/T)$ $F_{c,Ar} = 0.4148$
N_2	$k_{N_2,0}(T)^a = 4.83 \times 10^{-27} T^{-1.81} \exp(-400.86\ \text{K}/T)$ $k_\infty(T)^b = 2.04 \times 10^{-12} T^{0.58} \exp(107.57\ \text{K}/T)$ $F_{c,N_2} = 0.4225$
H_2O	$k_{H_2O,0}(T)^a = 4.80 \times 10^{-27} T^{-1.42} \exp(-337.68\ \text{K}/T)$ $k_\infty(T)^b = 2.04 \times 10^{-12} T^{0.58} \exp(107.57\ \text{K}/T)$ $F_{c,H_2O} = 0.4872$

[a] unit: $\text{cm}^6\text{molec}^{-2}\text{s}^{-1}$;
[b] unit: $\text{cm}^3\text{molec}^{-1}\text{s}^{-1}$;
[c] all fits agree with 1D-ME calculations within 23% for all temperatures from 500 – 3000 K and all pressures from the low- to high-pressure limit.

Table 5
Temperature-dependent energy-transfer parameters from 1D-ME model.

	$\langle\Delta E_d\rangle_i$ (cm^{-1})	Z_i (10^{-10} cm^3 molec^{-1} s^{-1})
Ar	$30.87 \times (T/298\,\text{K})^{1.194}$	$0.230 \times T^{0.393} \times \exp(81.070\,\text{K}/T)$
N_2	$40.38 \times (T/298\,\text{K})^{1.097}$	$0.257 \times T^{0.395} \times \exp(85.036\,\text{K}/T)$
H_2O	$102.47 \times (T/298\,\text{K})^{1.529}$	$2.604 \times T^{0.165} \times \exp(30.378\,\text{K}/T)$

Table 6
Single Troe expression of 1D-ME calculations with third-body efficiencies.

$k_{M,0}(T)^a = 1.26 \times 10^{-27} T^{-1.67} \exp(-438.48\,\text{K}/T)$
$k_\infty(T)^b = 2.04 \times 10^{-12} T^{0.58} \exp(107.57\ \text{K}/T)$
$F_c = 0.4148$
$\epsilon_{N_2} = 1.53,\ \epsilon_{H_2O} = 22.56$

[a] unit: $\text{cm}^6\text{molec}^{-2}\text{s}^{-1}$;
[b] unit: $\text{cm}^3\text{molec}^{-1}\text{s}^{-1}$.

In the interim, the title reaction would likely be best represented as a single Troe expression (Table 6) for M = Ar, with (as required within the current implementations of the single Troe expression) T- and P-independent third-body efficiencies for each i, $\epsilon_i = k_{i,0}/k_{M,0}$ of 1.53 for $i = N_2$ and 22.56 for $i = H_2O$ – since most combustion codes implement this expression using a mixture rule similar to LMR,R. This of course comes at the expense of not being able to represent the unique T and P dependence of each i (introducing another ~25% uncertainty for each i in addition to the ~25% fitting errors for the reference bath gas, Ar).

Altogether, considering the sensitivity of the ME results to uncertainties in angular momentum transfer (> ~20%), limitations of the usual Troe formula in representing P dependence for a pure bath gas [50] (~20%, cf. Table 4), other uncertainties in experimental interpretations (e.g. secondary reactions), and above-mentioned limitations in the ability to represent T, P, and $\underline{X}$ dependence, uncertainties of 50% or more in the expression presented in Table 6 would not be unexpected.

3.2. The path forward

Achieving lower uncertainties for the title reaction in kinetic modeling would likely require both (1) improved quantification of $k(T, P, \underline{X})$ over broad ranges of T, P, and $\underline{X}$ and (2) improved abilities to represent $k(T, P, \underline{X})$ over broad ranges of T, P, and $\underline{X}$ in combustion codes. With regard to (1), a priori 2D-ME calculations for combustion-relevant bath gases, high-accuracy experiments over wider ranges of T, P, and $\underline{X}$, and/or combining theoretical and experimental data within frameworks that can account for other experimental interpretation uncertainties (e.g. secondary reactions, physical model parameters) [51–53] would be worthwhile.

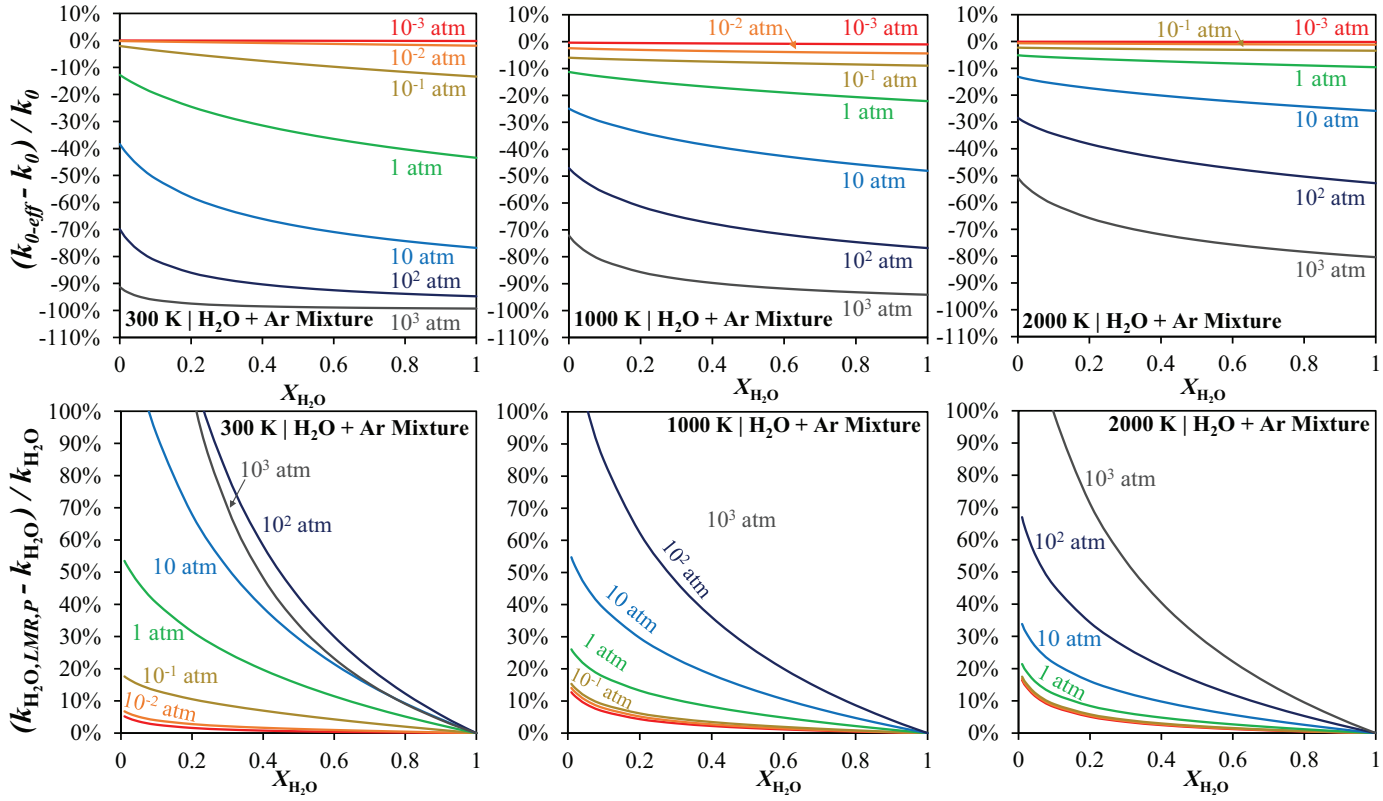

Fig. 2. 1D-ME calculated deviations of applying "effective" low-pressure limit (top row) and classic linear mixture rule (bottom row) in deriving bath-gas-specific rate constants in H_2O/Ar mixture at various (T, P, $\underline{X}$) conditions.

With regard to (2), incorporation of more accurate mixture rules (such as LMR,R and NMR,R with uncertainties in representing the title reaction within ~10% and 3%, respectively [34]) [34–36] into combustion codes [31,32,54,55] would be worthwhile. Furthermore, our recent results [56] suggest that new mixture rules may still be needed to describe the coupled kinetics of the title reaction and related chemically termolecular reactions (H + O_2 + H/O/OH) [57].

3.3. Recommendations for future experiments

With regard to future experiments, above all else, we recommend that future experimental studies report $k(T, P, \underline{X})$, the pseudo-second-order rate constant for H + O_2 ↔ HO_2, for each T, P, and $\underline{X}$ condition. (Of course, it would be most useful for studies to report the raw data to allow for the data to be reinterpreted in light of any new information about secondary reactions and experimental uncertainties in addition to assumptions regarding the title reaction, but the present discussion focuses on suggestions for reporting derived rate constants for the title reaction.) If one were to find $k(T, P, \underline{X})$ by fitting measurements at constant T/P/$\underline{X}$ conditions using a kinetic model, one would write the reaction simply as "H + O_2 ↔ HO_2" in a CHEMKIN or CANTERA input file and fit the preexponential factor at that condition to give $k(T, P, \underline{X})$, which could then be tabulated at various T, P, and $\underline{X}$ conditions of the experiments. In such a way, any uncertainties introduced in the interpretations of the data due to the assumption of k being in the low-pressure limit and/or following the classic linear mixture rule (LMR,P) would be avoided entirely.

If one is interested in performing experiments to derive $k_{A,0}(T)$ and $k_{H_2O,0}(T)$, one could choose experimental conditions to limit uncertainties due to the low-pressure limit and linear mixture rule assumptions. In that regard, the present 1D-ME model can be used to estimate the potential errors due to both assumptions over broad ranges of P and X_{H_2O}. Figure 2 shows the deviation from the low-pressure limit and the error in extracting $k_{H_2O}(T, P)$ from $k(T, P, \underline{X})$ via the linear mixture rule (LMR,P), calculated from the 1D-ME over broad ranges of P and X_{H_2O}. In general, the potential errors due to the two assumptions are lowest at low pressures; and potential errors due to the linear mixture rule are lowest for high H_2O mole fractions. For example, according to the ME model, if high-temperatures experiments were to be conducted for $P <$ 0.1 atm (or $P <$ 0.01 atm) for a H_2O/Ar mixture with $X_{H_2O} >$ 0.2 (or $X_{H_2O} >$ 0.25), the errors due to the low-pressure limit assumption and classic linear mixture rule could each be limited to ~10% (or ~5%).

Of course, since the title reaction is not in the low-pressure limit under many combustion-relevant conditions, high-accuracy experiments would be worthwhile across broad ranges of T, P, and $\underline{X}$ to ensure accurate quantification of k through the intermediate falloff regime (i.e. higher pressures). Given current limitations in combustion codes, this would be best accomplished by fitting $k(T, P, \underline{X})$ as discussed above. If one were interested in deriving the parameters for a Troe expression of the data, this would be best accomplished by fitting the parameters within LMR,R or NMR,R [34–36] (external to current codes) to the derived k or, with reduced fidelity to the unique T and P dependence of each i, using a single Troe expression within codes that implement a mixture rule similar to LMR,R (internal to current codes). The former has the advantage of enabling more accurate representations that can be used in future combustion codes; the latter has the advantage of enabling self-consistent representations for current combustion codes.

4. Conclusions

Master equation (ME) calculations for the title reaction were performed using a 1D-ME model with parameters chosen to yield rate constants consistent with reported data from recent high-precision studies of the title reaction. This model was then

used to estimate the potential errors in the derived $k_{i,0}(T)$ due to the assumption that the reaction is in the low-pressure limit and follows the classic linear mixture rule. Interestingly, the estimated errors due to the low-pressure limit assumption, $k_{0\text{-eff}}(T, P, \underline{X})/k_0(T, \underline{X})$, of ~5%, ~10-15%, and ~30% for the experimental conditions representative of [20,22], and [24] are comparable to reported uncertainties of 3–10%, 30%, and 12–19%. Similarly, the errors due to the assumed mixture rule in deriving H_2O-specific rate constants, $k_{H_2O}(T, P)$, from $k(T, P, \underline{X})$, of ~5%, ~15-20%, and ~40-45% for conditions representative of [20,22], and [24] are also comparable to reported uncertainties. Comparison of the ME model results for the variation of the derived rate constants across typical ranges of experimental conditions relative to experimental precision reveals that these potential errors, while significant, would have been imperceptible experimentally.

Further comparisons of the 1D-ME model results to those from an alternative one-dimensional model, the so-called 2D/φ-ME model, (performed here) and an a priori 2D-ME model [5,48] suggest that even the present 1D-ME interpretation of the experimental data is subject to uncertainties in the treatment of angular momentum that are not insignificant. Still, the present 1D-ME calculations can be viewed as an alternative interpretation of the experimental data (and provide an indication of the additional uncertainties in the experimental interpretations due to assumptions in the analysis). Furthermore, available representations of mixture effects for pressure-dependent reactions in current combustion codes introduce additional uncertainties in the representation of the 1D-ME-model-calculated rate constants.

Reducing uncertainties for the title reaction in kinetic modeling will require both (1) improved quantification of $k(T, P, \underline{X})$ over broad ranges of T, P, and $\underline{X}$ and (2) improved abilities to represent $k(T, P, \underline{X})$ over broad ranges of T, P, and $\underline{X}$ in combustion codes.

Until then, the above results suggest that both falloff and mixture effects are now significant uncertainty sources and should be considered in future uncertainty analysis of experimentally derived $k_{A,0}(T)$ and $k_{H_2O,0}(T)$. Likewise, until improved mixture rules [34–36] can be incorporated in combustion codes, treatment of the $T/P/\underline{X}$ dependence in kinetic models constitutes a significant structural uncertainty [51] (of up to ~90% [34]). Future mixture rules will also need to describe the coupled kinetics of termolecular association reactions (such as the title reaction) and related chemically termolecular reactions [57,58] (such as H + O_2 + H/O/OH) [56].

Finally, the present results suggest the advantages of different protocols for reporting experimental data for rate constants of pressure-dependent reactions. Namely, it is recommended that experimentally determined pseudo-second-order rate constants, $k(T, P, \underline{X})$, for H + O_2 ↔ HO_2 for the experimental temperature, pressure, and mixture composition (which are independent of low-pressure limit and mixture rule assumptions) be reported (to avoid the uncertainties due to these assumptions entirely). Some recommendations were also provided for future experimental studies that aim to determine low-pressure limit rate constants for various bath gases and/or derive parameters within Troe expressions of experimental data.

Declaration of Competing interest

The authors declare that they have no known competing financial interests or personal relationships that could have appeared to influence the work reported in this paper.

Acknowledgments

This work was supported by the National Science Foundation Combustion and Fire Systems program (CBET-1706252) and the Donors of the American Chemical Society Petroleum Research Fund through a Doctoral New Investigator award (PRF-56409-DNI-6).

Supplementary material

Supplementary material associated with this article can be found, in the online version, at doi:10.1016/j.combustflame.2019.11.041

References

[1] C.N. Hinshelwood, A.T. Williamson, The reaction between hydrogen and oxygen, Clarendon Press, Oxford, 1934.
[2] N.N. Semenov, Chemical kinetics and chain reactions, Clarendon Press, Oxford, 1935.
[3] L.S. Kassel, The kinetics of homogenous gas reactions, The Chemical Catalog Company, Inc., New York, 1932.
[4] C.K. Westbrook, F.L. Dryer, Chemical kinetics and modeling of combustion processes, Sym. (Int.) Combust. 18 (1981) 749–767.
[5] S.J. Klippenstein, From theoretical reaction dynamics to chemical modeling of combustion, Proc. Combust. Inst. 36 (2017) 77–111.
[6] H.J. Curran, Developing detailed chemical kinetic mechanisms for fuel combustion, Proc. Combust. Inst. 37 (2019) 57–81.
[7] F. Lindemann, S. Arrhenius, I. Langmuir, N. Dhar, J. Perrin, W.M. Lewis, Discussion on "the radiation theory of chemical action", Trans. Faraday Soc. 17 (1922) 598–606.
[8] C.N. Hinshelwood, On the theory of unimolecular reactions, Proc. R. Soc. Lond, Ser. A 113 (763) (1926) 230–233.
[9] D.C. Tardy, B.S. Rabinovitch, Intermolecular vibrational energy transfer in thermal unimolecular systems, Chem. Rev. 77 (3) (1977) 369–408.
[10] J. Troe, Predictive possibilities of unimolecular rate theory, J. Phys. Chem. 83 (1) (1979) 114–126.
[11] R.X. Fernandes, K. Luther, J. Troe, V.G. Ushakov, Experimental and modelling study of the recombination reaction H + O_2 (+M) → HO_2 (+M) between 300 and 900 K, 1.5 and 950 bar, and in the bath gases M = He, Ar, and N_2, Phys. Chem. Chem. Phys. 10 (2008) 4313–4321.
[12] J.A. Miller, S.J. Klippenstein, Master equation methods in gas phase chemical kinetics, J. Phys. Chem. A 110 (2006) 10528–10544.
[13] A.W. Jasper, K.M. Pelzer, J.A. Miller, E. Kamarchik, L.B. Harding, S.J. Klippenstein, Predictive a priori pressure-dependent kinetics, Science 346 (6214) (2014) 1212–1215.
[14] A. Matsugi, Origin of bath gas dependence in unimolecular reaction rates, J. Phys. Chem. A 123 (4) (2019) 764–770.
[15] S.R. Sellevag, Y. Georgievskii, J.A. Miller, The temperature and pressure dependence of the reactions H + O_2 (+M) → HO_2 (+M) and H + OH (+M) → H_2O (+M), J. Phys. Chem. A 112 (23) (2008) 5085–5095.
[16] M.A.A. Clyne, B.A. Thrush, R.G.W. Norrish, Rates of elementary processes in the chain reaction between hydrogen and oxygen II. Kinetics of the reaction of hydrogen atoms with molecular oxygen, Proc. Roy. Soc. A. 275 (1963) 559–574.
[17] R. Getzinger, L. Blair, Recombination in the hydrogen-oxygen reaction: A shock tube study with nitrogen and water vapour as third bodies, Combust. Flame 13 (1969) 271–284.
[18] K.J. Hsu, J.L. Durant, F. Kaufman, Rate constants for atomic hydrogen + oxygen + M at 298 K for M = helium, nitrogen, and water, J. Phys. Chem. 91 (1987) 1895–1899.
[19] K.L. Carleton, W.J. Kessler, W.J. Marinelli, Hydrogen atom + oxygen + M (= N_2, H_2O, Ar) three-body rate coefficients at 298–750 K, J. Phys. Chem. 97 (1993) 6412–6417.
[20] P.J. Ashman, B.S. Haynes, Rate coefficient of H + O_2+ M → HO_2+ M (M = H_2O, N_2, Ar, CO_2), Sym. (Int.) Combust. 27 (1998) 185–191.
[21] R.W. Bates, D.M. Golden, R.K. Hanson, C.T. Bowman, Experimental study and modeling of the reaction H+O_2+M → HO_2+M (M = Ar, N_2, H_2O) at elevated pressures and temperatures between 1050 and 1250 K, Phys. Chem. Chem. Phys. 3 (2001) 2337–2342.
[22] J.V. Michael, M.C. Su, J.W. Sutherland, J.J. Carroll, A.F. Wagner, Rate constants for H + O_2 + M → HO_2 + M in seven bath gases, J. Phys. Chem. A 106 (2002) 5297–5313.
[23] J.D. Mertens, D.M. Kalitan, A.B. Barrett, E.L. Petersen, Determination of the rate of H+O_2+M → HO_2+M (M=N_2, Ar, H_2O) from ignition of syngas at practical conditions, Proc. Combus. Inst. 32 (2009) 295–303.
[24] J. Shao, R. Choudhary, A. Susa, D.F. Davidson, R.K. Hanson, Shock tube study of the rate constants for H + O_2 + M → HO_2 + M (M = Ar, H_2O, CO_2, N_2) at elevated pressures, Proc. Combust. Inst. 37 (2019) 145–152.
[25] S.S. Vasu, D.F. Davidson, R.K. Hanson, Shock tube study of syngas ignition in rich CO_2 mixtures and determination of the rate of H + O_2+ CO_2 → HO_2+ CO_2, Energy Fuels 25 (2011).
[26] F.M. Haas, Studies of small molecule reactions foundational to combustion chemistry, Princeton University, 2016 (Ph.D. thesis).
[27] R. Choudhary, J.J. Girard, Y. Peng, J. Shao, D.F. Davidson, R.K. Hanson, Measurement of the reaction rate of H+O_2+M → HO_2+M, for M= Ar, N_2, CO_2, at high temperature with a sensitive oh absorption diagnostic, Combust. Flame 203 (2019) 265–278.

[28] A.C.A. Lipardi, J.M. Bergthorson, G. Bourque, NOx emissions modeling and uncertainty from exhaust-gas-diluted flames, J. Eng. Gas Turb. Power 138 (2015) 051506.
[29] P. Sabia, G. Sorrentino, P. Bozza, G. Ceriello, R. Ragucci, M. de Joannon, Fuel and thermal load flexibility of a MILD burner, Proc. Combust. Inst. 37 (2018) 4547–4554.
[30] J.E. Dove, S. Halperin, S. Raynor, Deviations from the linear mixture rule in nonequilibrium chemical kinetics, J. Chem. Phys. 81 (1984) 799–811.
[31] R.J. Kee, F.M. Rupley, J.A. Miller, Chemkin-II: a Fortran chemical kinetics package for the analysis of gas-phase chemical kinetics, 1989.
[32] D.G. Goodwin, H.K. Moffat, R.L. Speth, Cantera: an object-oriented software toolkit for chemical kinetics, thermodynamics, and transport processes, 2017. Version 2.3.10.
[33] J. Troe, Mixture rules in thermal unimolecular reactions, Ber. Bunsenges. Phys. Chem. 84 (1980) 829–834.
[34] M.P. Burke, R. Song, Evaluating mixture rules for multi-component pressure dependence: H+O_2 (+M)=HO_2 (+M), Proc. Combust. Inst. 36 (2017) 245–253.
[35] L. Lei, M.P. Burke, Evaluating mixture rules and combustion implications for multi-component pressure dependence of allyl + HO_2 reactions, Proc. Combust. Inst. 36 (2017) 245–253.
[36] L. Lei, M.P. Burke, Bath gas mixture effects on multichannel reactions: Insights and representations for systems beyond single-channel reactions, J. Phys. Chem. A 123 (2019) 631–649.
[37] Y. Tao, G.P. Smith, H. Wang, Critical kinetic uncertainties in modeling hydrogen/carbon monoxide, methane, methanol, formaldehyde, and ethylene combustion, Combust. Flame 195 (2018) 18–29.
[38] C. Olm, T. Varga, Éva Valkó, H.J. Curran, T. Turányi, Uncertainty quantification of a newly optimized methanol and formaldehyde combustion mechanism, Combust. Flame 186 (2017) 45–64.
[39] N.A. Slavinskaya, M. Abbasi, J.H. Starcke, R. Whitside, A. Mirzayeva, U. Riedel, W. Li, J. Oreluk, A. Hegde, A. Packard, M. Frenklach, G. Gerasimov, O. Shatalov, Development of an uncertainty quantification predictive chemical reaction model for syngas combustion, Energy Fuels 31 (2017) 2274–2297.
[40] R.K. Hanson, D.F. Davidson, Recent advances in laser absorption and shock tube methods for studies of combustion chemistry, Prog. Energy Combust. Sci. 44 (2014) 103–114.
[41] A.A. Konnov, Yet another kinetic mechanism for hydrogen combustion, Combust. Flame 203 (2019) 14–22.
[42] Y. Georgievskii, J.A. Miller, M.P. Burke, S.J. Klippenstein, Reformulation and solution of the master equation for multiple-well chemical reactions, J. Phys. Chem. A 117 (2013) 12146–12154.
[43] L.B. Harding, S.J. Klippenstein, H. Lischka, R. Shepard, Comparison of multireference configuration interaction potential energy surfaces for H + $O_2 \rightarrow$ HO_2: The effect of internal contraction, Theor. Chem. Acc. 133 (2014) 1–7.
[44] A.I. Maergoiz, E.E. Nikitin, J. Troe, V.G. Ushakov, Classical trajectory and adiabatic channel study of the transition from adiabatic to sudden capture dynamics. III. Dipoledipole capture, J. Chem. Phys. 105 (15) (1996) 6277–6284.
[45] P. Paul, J. Warnatz, A re-evaluation of the means used to calculate transport properties of reacting flows, Sym. (Int.) Combust. 27 (1) (1998) 495–504.
[46] S.J. Klippenstein, A.F. Wagner, R.C. Dunbar, D.M. Wardlaw, S.H. Robertson, Variflex, version 1.00, Argonne National Laboratory, Argonne, IL, 1999.
[47] A.W. Jasper, J.A. Miller, S.J. Klippenstein, Collision efficiency of water in the unimolecular reaction CH_4 (+H_2O) $\leftrightarrows$ CH_3 + H (+H_2O): One-dimensional and two-dimensional solutions of the low-pressure-limit master equation, J. Phys. Chem. A 117 (47) (2013) 12243–12255.
[48] M. Verdicchio, A.W. Jasper, M.P. Burke, K.M. Pelzer, J.A. Miller, S.J. Klippenstein, A priori pressure-dependent kinetics for the H + O_2 (+M) $\rightarrow$ HO_2 (+M) reaction, manuscript in preparation (2019).
[49] R.G. Gilbert, K. Luther, J. Troe, Theory of thermal unimolecular reactions in the fall-off range. II. Weak collision rate constants, Ber. Bunsenges. Phys. Chem. 87 (2) (1983) 169–177.
[50] J. Troe, V.G. Ushakov, Revisiting falloff curves of thermal unimolecular reactions, J. Chem. Phys. 135 (5) (2011) 054304.
[51] M.P. Burke, Harnessing the combined power of theoretical and experimental data through multiscale informatics, Int. J. Chem. Kinet. 48 (2016) 212–235.
[52] M.P. Burke, S.J. Klippenstein, L.B. Harding, A quantitative explanation for the apparent anomalous temperature dependence of OH+HO_2=H_2O+O_2 through multi-scale modeling, Proc. Combust. Inst. 34 (1) (2013) 547–555.
[53] M.P. Burke, C.F. Goldsmith, S.J. Klippenstein, O. Welz, H. Huang, I.O. Antonov, J.D. Savee, D.L. Osborn, J. Zádor, C.A. Taatjes, L. Sheps, Multiscale informatics for low-temperature propane oxidation: Further complexities in studies of complex reactions, J. Phys. Chem. A 119 (28) (2015) 7095–7115.
[54] H. Pitsch, FlameMaster: A C++ computer program for 0D combustion and 1D laminar flame calculations, 1998. Version 3.3.10.
[55] A. Cuoci, A. Frassoldati, T. Faravelli, E. Ranzi, Opensmoke++: An object-oriented framework for the numerical modeling of reactive systems with detailed kinetic mechanisms, Comput. Phys. Commun. 192 (2015) 237–264.
[56] L. Lei, M.P. Burke, Reaction kinetics of chemically termolecular reactions: pressure dependence, 11th U.S. National Meeting of the Combustion Institute (2019).
[57] M.P. Burke, S.J. Klippenstein, Ephemeral collision complexes mediate chemically termolecular transformations that affect system chemistry, Nat. Chem. 9 (2017) 1078–1082.
[58] M.C. Barbet, K. McCullough, M.P. Burke, A framework for automatic discovery of chemically termolecular reactions, Proc. Combust. Inst. 37 (1) (2019) 347–354.